Generation of third-order spherical and coma aberrations by use of radially symmetrical fourth-order lenses

N. López-Gil

Section of Neurobiology and Behavior, Cornell University, Ithaca, New York 14853-2702 and Laboratorio de Óptica, Departamento de Física, Universidad de Murcia, 30071 Murcia, Spain

H. C. Howland

Section of Neurobiology and Behavior, Cornell University, Ithaca, New York 14853-2702

B. Howland

4913 Regent Street, Madison, Wisconsin 53705

N. Charman

Department of Optometry and Vision Science, University of Manchester Institute of Science and Technology, P.O. Box 88, Manchester, M60 1QD, UK

R. Applegate

Department of Ophthalmology, University of Texas Health Science Center at San Antonio, San Antonio, Texas 78284-6230

Received December 24, 1997; revised manuscript received April 28, 1998; accepted May 1, 1998

We have extended the method of Alvarez [J. Am. Optom. Assoc. **49**, 24 (1978)] to generate a variable magnitude of third-order spherical and/or coma aberration by using a combination of fourth-order plates with a magnification system. The technique, based on the crossed-cylinder aberroscope, is used to measure the wave-front aberration generated by the plates. The method has been applied to correct the third-order spherical aberration generated by an artificial eye as well as the coma produced by a progressive addition ophthalmic lens. The simplicity of the method and its relatively low cost make it attractive for partial correction of the aberrations of the eye. © 1998 Optical Society of America [S0740-3232(98)03709-0]

OCIS codes: 220.1000, 220.1010, 220.4830, 220.0220, 170.4460, 170.4470.

1. INTRODUCTION

Several methods have been employed in the past two decades to measure the monochromatic aberrations of the human eye. Most are objective methods based on the analysis of light that leaves the eye after reflection by the retina. The subjective method, using a crossed-cylinder aberroscope as described by Howland and Howland,[1] has been made objective by the introduction of an ophthalmoscopic pathway that records the image of a distorted grid on the retina.[2] The information given by the distortion of the grid when the light traverses the eye toward the retina is used in this method. The double-pass method analyzes the image of a point source, taking into account the fact that it is affected in both passes,[3] while the technique that employs a Hartmann–Shack detector[4] bases its analysis on the returned wave front of the light that passes through the ocular media when the light is leaving the eye.

With the advent of techniques for measuring the wave aberration of the human eye, it has become desirable to develop optical systems that generate the appropriate aberration to correct the one present in the optical system of the eye. In the past, much effort has been directed at eliminating high-order aberrations from optical systems by optimizing design, often with the help of computers. As an example, the Schmidt negative fourth-order corrector plate was designed to remove the spherical aberration from a spherical mirror.[5] Generally, optical engineers strive to remove monochromatic aberrations from their optical systems by refining the (usually spherical) shapes of their surfaces, the refractive indices of their lenses, and the placement of the optical elements. However, several researchers have used optical devices such as lenses, to generate a specific amount of chromatic aberration,[6,7] or contact lenses, to produce third-order spherical aberration.[8] They have analyzed the effects of these lenses on vision and, in particular, on dynamic events such as accommodation. Although those techniques have been successfully applied with interesting results, they are capable of inducing only constant amounts of aberra-

0740-3232/98/092563-09$15.00

tion. A variable amount of second- and third-order aberrations can be generated by arrangements composed of plano–spherical or cylindrical lenses.[9,10] The advantage of those setups is the inexpensiveness of their compounds, but, because of the large number of elements, their perfect alignment is rather complicated. Two relatively simple techniques have been applied recently to compensate the wave aberration. The first is based on the use of deformable mirrors, typically used in astronomy, which allow the recording of a high-quality fundus image.[11] The second uses a liquid-crystal device, which locally varies the phase of the wave front and, in so doing, compensates the wave-front error by transmission.[12] Although these technologies have a great potential in generating and compensating different amounts of wave aberrations, they are rather expensive, at least at the present time.

In this paper we extend the method of Alvarez[13] to generate third-order spherical and coma aberrations as a simple and more economical means of correcting some of the aberrations of the eye. The solutions presented here employ wave aberration plates of fixed value, which, when combined with other wave aberration plates or optical elements, give variable amounts of coma and/or spherical aberration. The method is applied to compensate the third-order spherical aberration of an artificial eye and the third-order coma of a progressive addition ophthalmic lens.

2. METHODS

In the plates that we used, the first surface is planar and the other has a radial symmetrical shape with the form $K(r^4)$. At the edge of a pupil with a 1-mm radius, a single plate generates a third-order spherical aberration (in terms of the Zernike expansion) of $(1000)(n-1)K/6$ μm (see the corresponding Zernike coefficient below). A variable amount of coma can be generated by displacement of just one of these plates perpendicular to the optical axis, but the spherical aberration remains, and tilt, astigmatism, and defocus will also appear. Moreover, the values of the latter aberrations increase as the second (astigmatism and defocus) or the third power (tilt) of the displacement. These undesired aberrations, especially the remaining third-order spherical, can be totally or partially avoided by a combination of two plates.

As a general example, when two plates with shapes $K_1(r^4)$ and $K_2(r^4)$ are combined and displaced a distance of h_1 and h_2, respectively, in the same direction (e.g., y) with respect to the optical axis (z direction), they produce a wave aberration

$$\begin{aligned} W(x, y) = 1000(n-1)\{&K_1[x^4 + (y + h_1)^4 \\ &+ 2x^2(y + h_1)^2] + K_2[x^4 + (y + h_2)^4 \\ &+ 2x^2(y + h_2)^2]\}, \end{aligned} \tag{1}$$

where it has been assumed that both plates are in proximity. This expression can be rewritten as

$$\begin{aligned} W(x, y) = 1000(n-1)\{&[K_1 + K_2](x^2 + y^2)^2 \\ &+ [4(K_1h_1 + K_2h_2)]y(x^2 + y^2) \\ &+ [2(K_1h_1^2 + K_2h_2^2)](x^2 + 3y^2) \\ &+ [4(K_1h_1^3 + K_2h_2^3)]y + (h_1^4 + h_2^4)\}, \end{aligned} \tag{2}$$

where the first, second, third, and fourth coefficients, in brackets, are related to third-order spherical aberration, coma along the Y axis, astigmatism with axis at 0° or 90°, and tilt along the X axis and piston, respectively.[14] Equation (2) can also be expressed in orthogonal functions, which are especially interesting if one wishes to correct a specific amount of aberration to minimize the wave-front variance. We can then convert the wave front in Eq. (1) to the equivalent Zernike expression[15] to obtain

$$\begin{aligned} W(x, y) = z_0 &+ z_2y + z_4(2x^2 + 2y^2 - 1) + z_5(y^2 - x^2) \\ &+ z_8(3x^2y + 3y^3 - 2y) + z_{12}(6x^4 + 6y^4 \\ &+ 12x^2y^2 - 6x^2 - 6y^2 + 1), \end{aligned} \tag{3}$$

where x and y are coordinates normalized to the pupil radius, r, over which the wave front is defined and the Zernike coefficients, z_i, are related to $K_{1,2}$ and $h_{1,2}$ as

$$\begin{aligned} z_0 &= A[(K_1h_1^4 + K_2h_2^4) + 2(K_1h_1^2 + K_2h_2^2)r^2 + 1/3(K_1 + K_2)r^4] && \text{(piston)}, \\ z_2 &= 4A[2/3(K_1h_1 + K_2h_2)r^3 + (K_1h_1^3 + K_2h_2^3)r] && \text{(tilt)}, \\ z_4 &= A[2(K_1h_1^2 + K_2h_2^2)r^2 + 1/2(K_1 + K_2)r^4] && \text{(defocus)}, \\ z_5 &= 2A(K_1h_1^2 + K_2h_2^2)r^2 && \text{(astigmatism)}, \\ z_8 &= (4A/3)(K_1h_1 + K_2h_2)r^3 && \text{(third-order coma)}, \\ z_{12} &= (A/6)(K_1 + K_2)r^4 && \text{(third-order spherical)}, \end{aligned}$$

where A is the constant $1000(n-1)$. In analyzing these coefficients, one can avoid the contribution of the astigmatism and certain amounts of defocus by using $h_1 = h_2 = 0$ or

$$K_1/K_2 = -(h_2/h_1)^2, \tag{4}$$

which forces K_1 and K_2 to have opposite signs. Under this condition, it is also possible to avoid the spherical aberration by giving K_1 and K_2 opposite values. In this particular case, the amount of third-order coma will vary linearly with the displacement of the plates, producing a value of $(8/3)AK_1h_1(r^3)$. The tilt produces a displacement only in the image plane, which does not pose a significant problem for isoplanatic systems. The plates induce a residual amount of defocus, $A(K_1 + K_2)r^4/2$, that can be avoided by use of the appropriate spherical lens, by

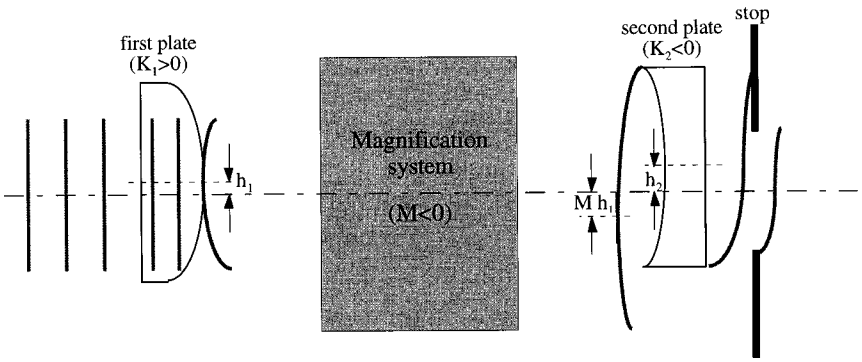

Fig. 1. Schematic views of the generation of a variable amount of third-order spherical and coma aberrations by use of a magnification system between two plates that are displaced with respect to the optical axis. The wave front generated by the first plate is magnified and projected onto the second plate.

means of a Badal system,[16] or with two Alvarez lenses.[13] Equation (4) and the restriction of no coma would give the trivial solution, where $K_1 = -K_2$ and $h_1 = h_2$. Thus the only way to obtain an image with spherical aberration and no coma is by using $h_1 = h_2 = 0$, which generates a constant spherical aberration with a value of $1/6A(K_1 + K_2)(r^4)$. There is an interesting effect when one uses two plates with opposite K values that are displaced in opposite sense. Here an extra displacement, Δh, of the ensemble of both plates keeps the spherical and coma aberrations unchanged but produces an astigmatism of $8AK_1h_1\Delta h(r^2)$.

If we want to generate a specific amount of spherical aberration, we can use a plate together with a magnification system that projects the enlarged image of a pupil at the plate into a stop with the same radius as that of the unmagnified pupil (see Fig. 1). The effect of such a system on the aberration will be the same as that of reducing the radius of the original wave-front aberration by the amount of magnification. The value of the spherical aberration will then decrease (in absolute value) with the fourth order of the magnification, so, in practical terms, it is only necessary to have a small range of magnification to produce a large range of that aberration. Taking into account the fact that the defocus necessary to balance the aberration would decrease (in absolute value) with the square of the magnification, one must modify the defocus each time a new magnification is used, to minimize the mean square of the wave-front aberration. For such a system, the value of the third-order spherical aberration varies with the fourth power of the radius, and K_1 should be replaced by K_1/M^4, with M being the value of the lateral magnification. The expression of the spherical aberration after the magnification is

$$z_{12} = A/6K_1(r/M)^4.$$

It may be desirable to correct the third-order spherical and coma aberrations at the same time. This can be done by use of a magnification system between two plates with opposite K values displaced somewhat with respect to the optical system, as shown in Fig. 1. Appendix A elaborates this possibility.

We present below the generation and the measurement of third-order spherical and coma aberrations by one or a combination of two plates, as well as two examples of partial correction of the wave-front aberration. The first example concerns the correction of the spherical aberration in an artificial eye. In the second example we correct the coma aberration presented in a progressive addition ophthalmic lens.

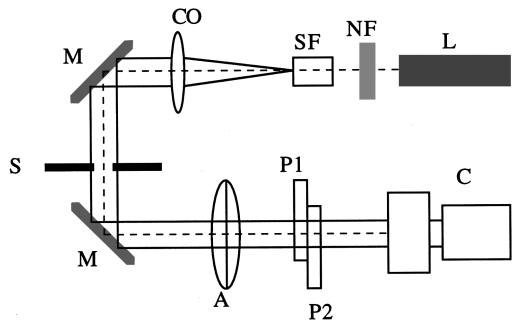

Fig. 2. Schematic view of the setup. *L*, He–Ne laser (632.8 nm); NF, neutral-density filter; SF, spatial filter (consisting of a microscope objective and a pinhole); CO, collimator; M, mirror; S, iris stop; A, aberroscope; P1 and P2, plates; C, CCD camera.

3. RESULTS

We used the setup shown in Fig. 2 to measure the aberration generated by one or a combination of plates, using a method based on the aberroscope.[17] In this case the aberroscope, A, consists of a grid mounted between two cylindrical lenses of ±5 diopters (D), whose axes are crossed at 90°. The grid is predistorted to produce a perfect square grid at the plate. The objective of the camera, C, has a focal length of 50 mm. The plates used are made in standard optical acrylic, poly(methyl methacrylate), and have an index of refraction of 1.4898 for the wavelength used (632.8 nm), a central thickness of 3 mm, a radius of 7 mm, and a K value that varies from -2.08×10^{-4} to 2.08×10^{-4} mm^{-3} in steps of 0.26×10^{-4}. (The plates were manufactured by Precision Lens Company, Flintshire, Wales, UK.)

Figures 3 and 4 show two examples of grid patterns that correspond to a pure spherical and a coma aberration, respectively. The grid spacing used was 1.23 mm. The point-spread functions (PSF's) produced by these wave aberrations are shown in the upper right-hand corners of the two figures. Figure 3 corresponds to a third-order spherical aberration generated by a plate with $K = -0.260 \times 10^{-4}$. In this case we found the smallest

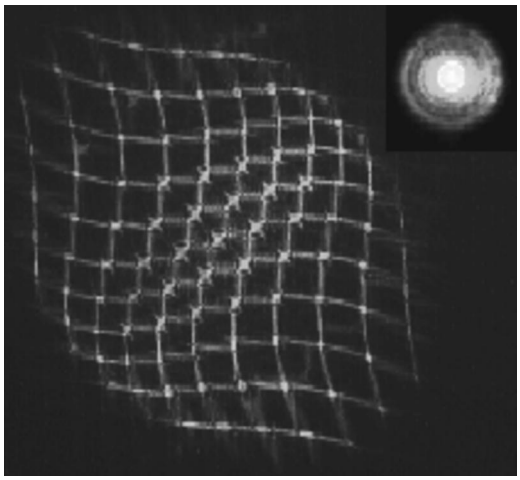

Fig. 3. Grid image recorded with a crossed-cylinder aberroscope of a negative third-order spherical aberration generated by a plate of $K = -0.260 \times 10^{-4}$. The PSF generated by the aberration is represented in the upper right-hand corner of the image.

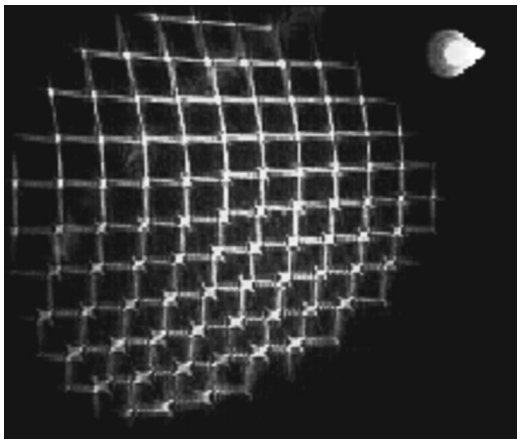

Fig. 4. Grid image recorded with a crossed-cylinder aberroscope of a negative horizontal (along the X axis) coma aberration generated by a combination of two plates with $K_1 = -K_2 = -0.260 \times 10^{-4}$ separated by a distance of 1 mm. The PSF generated by the aberration is represented in the upper right-hand corner of the image.

PSF by defocusing the objective camera to balance the spherical aberration produced by the plate. The latter can be seen in the image of the grid, which is fitted in the center but not at the periphery. Figure 4 represents the third-order coma along the X axis that is generated with a combination of two plates, $K_1 = -K_2 = -0.260 \times 10^{-4}$, displaced horizontally 0.5 mm to each other in opposite directions.

Table 1 shows the measurements of third-order spherical and coma aberration coefficients expressed in micrometers for a pupil radius of 3 mm. The values have been obtained by use of three different plates singly or in combinations of two displaced to each other. See Table 1 for specific values of K and h. To generate coma along the X axis, we use two micrometric positioners to displace the plates in the horizontal direction. Table 1 also shows the results of spherical and coma aberration values after computer simulation with commercial software (ZEMAX, Focus Software, Inc.) and the theoretical values obtained by use of Eq. (3).

A. Correction of the Third-Order Spherical Aberration Generated by an Artificial Eye

We used the setup shown in Fig. 5 to record the distorted grid after a double pass through an artificial eye. In this case we used a magnification system (MS) to project a square grid (1.23-mm grid spacing) in the entrance pupil of the eye as well as the effect of the crossed cylinder. The image recorded [Fig. 6(a)] clearly shows the presence of third-order spherical aberration as revealed in the computerized analysis (value of 0.181 μm for a pupil diameter of 6 mm). Because this value is very close to the spherical aberration generated by a plate with a K value of 0.26×10^{-4} (see Table 1), we correct the aberration by using a plate with this K value together with a trial lens of +1 D placed in front of the artificial eye to partially balance the aberration. Figure 6(b) shows the grid image

Table 1. Measurements and Calculations of Third-Order Spherical and Coma Aberrations of Wave Plates[a]

Aberration	Value	Measured (μm)	Simulated (μm)	Theoretical (μm)
Spherical				
K (mm^{-3})	0.260×10^{-4}	0.170	0.172	0.172
	0.521×10^{-4}	0.349	0.344	0.344
	1.041×10^{-4}	0.682	0.689	0.689
Coma along X axis				
$h_{1,2}$ (mm)	0.5	0.458	0.458	0.458
	1	0.815	0.917	0.917
	1.5	1.167	1.375	1.375

[a] Values in micrometers of optical path difference at pupil edge of third-order spherical and coma aberrations for a pupil radius of 3 mm were obtained by measurement with the crossed-cylinder aberroscope, by computer simulation, and by theoretical calculations. Two plates with $K_1 = -K_2 = 0.260 \times 10^{-4}$ were used in the coma generation.

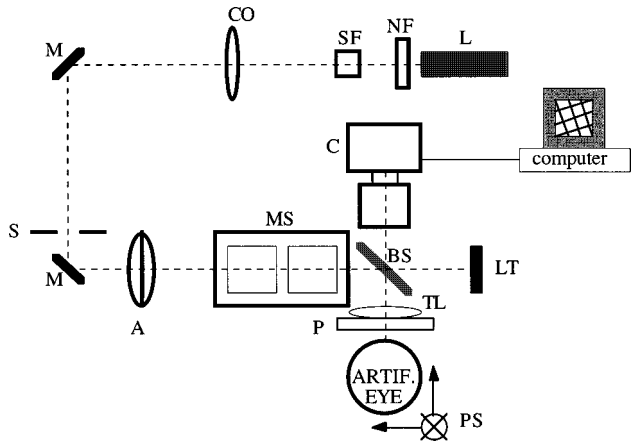

Fig. 5. Schematic view of the setup used to measure and correct the spherical aberration of an artificial eye. L, He–Ne laser (632.8 nm); NF, neutral-density filter; SF, spatial filter; CO, collimator; M, mirror; S, iris stop; A, aberroscope; MS, magnification system ($M = 1$); BS, beam splitter; P, plate; TL, trial lens; PS, positioners; LT, light trapper; C, CCD camera.

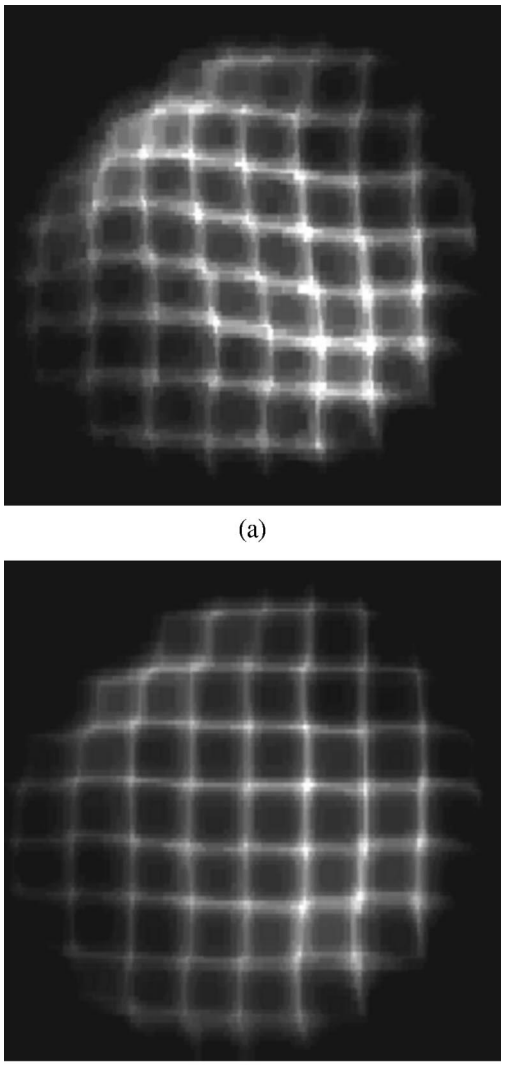

Fig. 6. Aberroscopic images recorded on an artificial eye (a) before and (b) after correction of the third-order spherical aberration by use of a plate with $K = -0.260 \times 10^{-4}$.

recorded after compensation. By comparison of the two images shown in Fig. 6 it can be seen that, after compensation, the grid is much less distorted, and the grid lines are better defined because the PSF has been improved and therefore causes less degradation of the image in both passes. When the plate is used for compensation, the value of the remaining spherical aberration is 0.005 μm. If we compute the difference in the values of the aberration found before and after compensation, we get 0.176 μm, which, as expected, is very close to the spherical aberration generated by the plate we used (see Table 1). A nonperfect match can be explained in terms of small errors in locating the crossed lines. The wave-front aberrations before and after correction for a pupil of 5 mm are shown in Fig. 7. The wave fronts show some asymmetries related to the presence of comalike aberration that results when the pupil of the artificial eye is not perfectly centered with respect to the axis of the measurement system. The reduction in the peak-to-valley value after correction is 36.7%.

B. Correction of the Third-Order Coma Aberration Generated by Progressive Addition Lens

We used a setup similar to the one presented in Fig. 2 to measure and correct the third-order coma aberration of a progressive addition ophthalmic lens (OD, 0 D; ADD, +2 D). In this case we used the same magnification system as shown in Fig. 5 to project the optical effect of the plates into the ophthalmic lens. In this setup the collimated light coming from the He–Ne laser passes through the plates, the magnification system ($M = -1$), the aberroscope, and the ophthalmic lens and finally arrives at the camera. The image of the distorted grid produced by an ophthalmic lens without any correction is shown in Fig. 8. The center of the image corresponds to a position halfway between the axis of far and near distance vision (gray circle in Fig. 9). It is well known that this kind of lens generates undesired astigmatism and coma, the values of which vary along the lens, as demonstrated in Fig. 8. Going from the top to the bottom in Fig. 8, the grid shape changes from an undistorted square grid in the upper part where there is no power to astigmatism at 0 deg (only the vertical lines tilt) to defocus in the lower part (both the vertical and the horizontal lines tilt) and coma (the horizontal lines curve). Figure 8 presents a large portion of the lens (diameter almost 2 cm) where astigmatism and coma vary from one part to another. To measure and compensate the third-order coma aberration, we

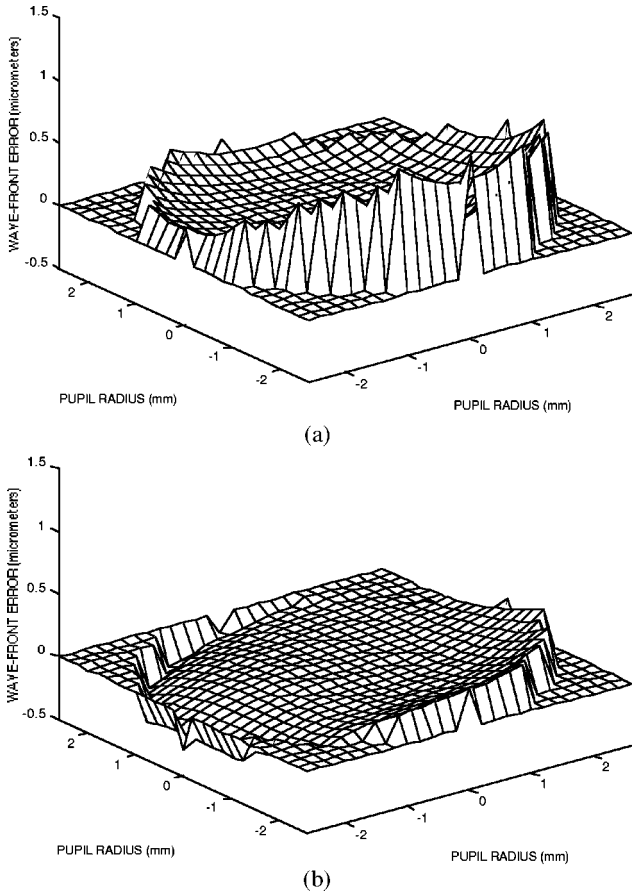

Fig. 7. Reconstruction of the wave-front error with the third- and fourth-order Taylor coefficients ($G-O$) obtained from the aberroscopic images of Fig. 5(a) before and (b) after correction of the third- and fourth-order spherical aberration.

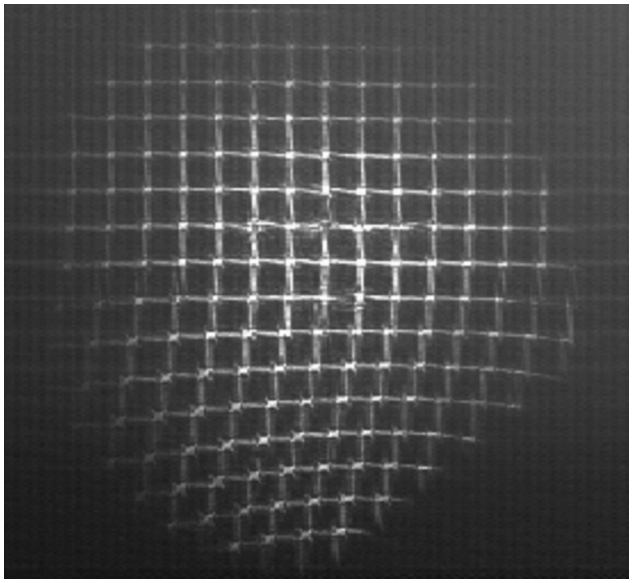

Fig. 8. Aberroscopic image of a progressive lens (OD, 0 D; ADD, +2 D). The field represented is 19.7 mm and is centered in the midpoint between far and near vision (see Fig. 9). The image recorded has been rotated and flipped for clarity. Note the orthogonality of the grid in the upper portion and the distortion (owing to defocus, astigmatism, and coma) in the lower portion.

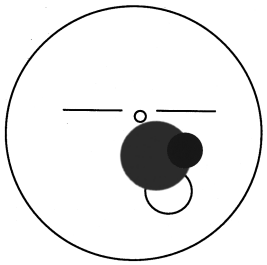

Fig. 9. Precise location on the progressive lens (OD, 0 D; ADD, +2 D) of the zones analyzed by the aberroscopic technique. The gray circle corresponds to the zone presented in Fig. 8. The black circle corresponds to the zones presented in Figs. 10(a) and 10(c). The small and large open circles represent the centers for far and near vision, respectively.

used a smaller pupil (8.4-mm diameter) centered more nasally with respect to the one shown in Fig. 8. The exact position is shown in Fig. 9 (black circle), and the grid recorded appears in Fig. 10(a). We then calculated the Zernike coefficients of that image for a 7×7 grid with the same grid spacing as used before. The values obtained indicate that the main aberration present was astigmatism, along with a relatively small amount of vertical (-0.417 μm) and horizontal (0.278-μm) coma. Spherical aberration was very small (-0.009 μm). These values are the coefficients of the Zernike terms[15] and express the deviation of the wave front from the reference sphere, in micrometers, at a radius of 4.2 mm. It is important to note that the values obtained represent the average coefficients for the analyzed pupil. They do not correspond exactly with those of a person with that pupil diameter who wears the lens, because in natural viewing the eye rotates, and the visual axis is not horizontal.[18]

We employed the values of the vertical and horizontal coma to correct those lens aberrations by using two plates

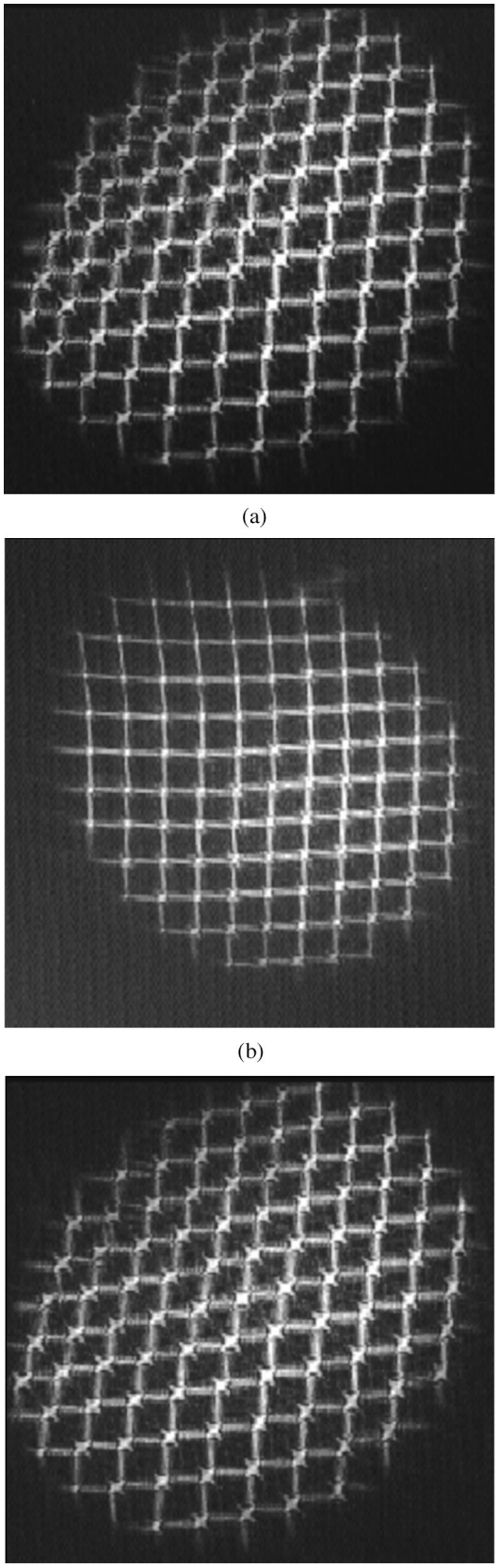

(a)

(b)

(c)

Fig. 10. Aberroscopic images recorded for a progressive ophthalmic lens (a) before correction of the third-order coma aberration, (b) with correction generated by the plates, and (c) after correction.

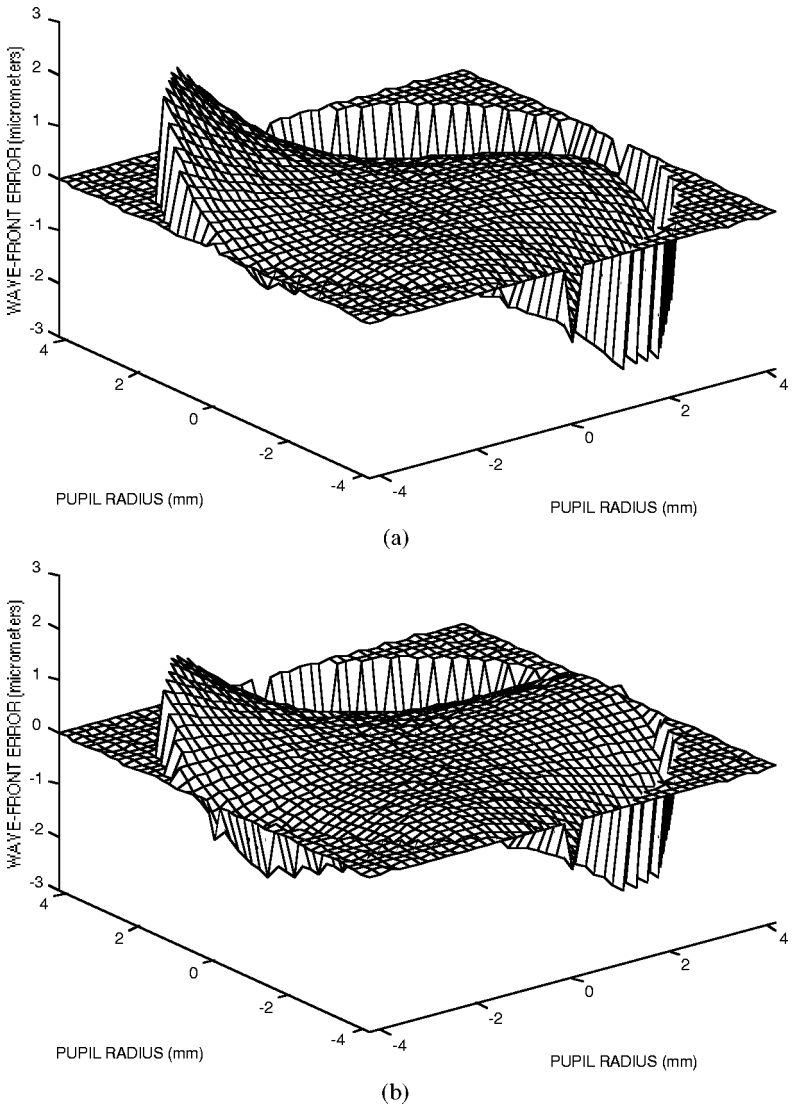

Fig. 11. Reconstruction of the wave-front error (a) before and (b) after correction of third-order coma aberration by use of the third- and fourth-order Taylor coefficients obtained from the aberroscopic images of Figs. 10(a) and 10(c), respectively.

with an opposite K value of 0.26×10^{-4} both mounted in a $X-Y$ microtranslator. Theoretically, the best compensation produced with the plates (in terms of the least wave-front variance) is obtained when the Taylor coefficients[1] that are generated (G', H', I', and J') have a value of

$$G' = I' = -\frac{3G + I}{4}, \quad H' = J' = -\frac{3J + H}{4},$$

where G, H, I, and J are the coefficients obtained without correction. We use those values to obtain the displacement of the plates. Figure 10(b) represents the grid produced when only the plates to correct the aberration are used, and Fig. 10(c) shows the image recorded after compensation. The latter shows straighter and more-parallel lines because of the correction. Figures 11(a) and 11(b) represent the wave-front errors generated with the Taylor values corresponding to third- and fourth-order coefficients[1] ($G-O$) calculated from the images obtained before and after correction, respectively. For a pupil of 4.2-mm radius, the wave-front error has been reduced after correction and the peak-to-valley value has been decreased by 30.7%.

4. DISCUSSION AND SUMMARY

We have presented a simple and relatively inexpensive method of generating third-order spherical aberration and coma. By combining one or two plates with a fourth-order radial–symmetrical surface and a magnification system we can produce a precise and variable range of those aberrations.

Theoretical calculation has shown that it is possible to generate a precise amount of coma or spherical aberration either alone or in combination. Experimental measurements made with a cross-cylinder aberroscope[1,2,17,19] of most of the aberrations generated agree well with the measurements obtained by computer simulation. In the case of the highest coma, however, we have found a difference of nearly 15% between the simulated and the measured values. Two sources of error can cause this

discrepancy. First, the PSF increases for large aberrations, thus increasing the error in locating the grid intersection. Second, small errors in the optical center of the plates with respect to the aberroscope axis are transformed into errors in the coma aberration, which increase with the aberration. The small differences found between theoretical and simulated data of the coma aberration are mainly due to the small layer of air remaining between the plates.

We have applied the method to successfully correct the third-order spherical aberration of an artificial eye. Correcting that aberration in both passes permits us not only to record an image of the undistorted grid but also to obtain a sharper image of the lines that form the grid. This technique can be applied to obtain retinal images of a distorted grid in eyes with a large amount of spherical aberration (i.e., after radial keratotomy). We have also used the crossed-cylinder aberroscope technique to measure, for the first time to our knowledge, the wave-front error of a progressive addition ophthalmic lens. Using a combination of two plates with opposite K values, we have partially corrected the asymmetrical aberration present in a nasal zone between the far and the near distance vision of the lens. In both cases we obtained an important reduction in the peak-to-valley wave front after correction.

This method could be used to generate the precise third-order spherical and/or coma aberration to compensate or augment these aberrations of the eye, making it possible to study whether these aberrations play an important role in vision. It is noteworthy that the values of spherical and coma aberration generated by the plates used are of the same order of magnitude as the one found in the human eye.[20] For instance, the mean value of balanced spherical aberration for a pupil of 3-mm radius found for different authors[20] is 0.324 μm, which is close to the spherical aberration that can be corrected by a plate with a K value of -0.521×10^{-4} mm^{-3} (see Table 1).

The use of the plates integrated in a system with a crossed-cylinder aberroscope would allow us to subjectively measure and compensate the third-order spherical and/or coma aberration. The main problem of this method (and virtually any other method that does not physically link the correction to the eye) is that of centering the plates with respect to the eye's optical axis. As pointed out above, when the plate is displaced, values of coma, astigmatism, defocus, and tilt appear. For a certain pupil radius, r, the displacement of a plate that generates the same root-mean-square (rms) coma aberration as the one generated by the spherical aberration correction plate is

$$h = \frac{r}{\sqrt{40}}.$$

For the astigmatism this displacement is bigger:

$$h = \frac{r}{(120)^{1/4}}.$$

So, for instance, for a pupil of 3-mm radius, the improvement in the root-mean-square aberration when spherical aberration is perfectly corrected is in vain if the plate is displaced by only 0.459 mm from the eye's optic axis, even assuming that the tilt and defocus also generated by the displacement of the plate are corrected.

APPENDIX A

With a magnification system between two displaced plates so that the wave front generated by the first plate is magnified and projected on the second one (see Fig. 1), it is possible to generate the desired amount of third-order spherical and coma aberrations. For such a system Eq. (2) remains the same, except that K_1 would be replaced by $K_1/(M^4)$ and h_1 would be replaced by Mh_1, with M being the value of the lateral magnification. Equation (2) therefore becomes

$$\begin{aligned} W(x, y) = 1000(n - 1)\{&[(1/M^4)K_1 + K_2](x^2 + y^2)^2 \\ &+ [(4/M^3)K_1h_1 + K_2h_2]y(x^2 + y^2) \\ &+ [(2/M^2)K_1{h_1}^2 + K_2{h_2}^2](x^2 + 3y^2) \\ &+ [(4/M)K_1{h_1}^3 + K_2{h_2}^3]y \\ &+ [(M^4){h_1}^4 + {h_2}^4]\}. \end{aligned}$$

The new equation for avoidance of astigmatism becomes

$$M = (h_1/h_2)(-K_1/K_2)^{1/2}.$$

In the case of combining plates with $K_1 = -K_2$, the displacements and the magnification necessary to avoid the astigmatism and to generate a specific value of third-order spherical (S) and coma (C) aberrations are

$$M = \left(\frac{AK_1}{6S + AK_1}\right)^{1/4}, \quad h_1 = \frac{3CM^3}{4AK_1(1 + M^2)},$$

$$h_2 = \frac{-3CM^2}{4AK_1(1 + M^2)}.$$

When one uses a system that is able to produce a magnification of $0.5 \leqslant M \leqslant 2.0$ (for instance, by modification of the focal length, by the same amount but in opposite directions, of two 75–150-mm zoom lenses) and two 14-mm diameter plates, the range of possible third-order spherical aberration generated for a pupil radius of 1 mm is $-0.156K_1A \leqslant S \leqslant 2.5K_1A$, and the variation in coma coefficient is $-56K_1A$ to $56K_1A$.

ACKNOWLEDGMENTS

This work was supported by National Institutes of Health grants EY02994 (to H. C. Howland) and EY08520 (to R. Applegate) and by a Spanish Ministerio de Educación y Cultura postdoctoral fellowship (to N. López-Gil).

Address correspondence to N. López-Gil, W-203 Seeley Mudd Hall, Section of Neurobiology and Behavior, Cornell University, Ithaca, N.Y. 14853-2702 [telephone, (607) 254-4314; e-mail, norberto@fcu.um.es].

REFERENCES

1. H. C. Howland and B. Howland, "A subjective method for the measurement of monochromatic aberrations of the eye," J. Opt. Soc. Am. A **67**, 1508–1518 (1977).
2. G. Walsh, W. N. Charman, and H. C. Howland, "Objective

technique for the determination of monochromatic aberrations of the human eye," J. Opt. Soc. Am. A **1**, 987–992 (1984).
3. J. Santamaría, P. Artal, and J. Bescós, "Determination of the point-spread function of the human eye using a hybrid optical–digital method," J. Opt. Soc. Am. A **4**, 1109–1114 (1987).
4. J. Liang, B. Grimm, S. Goelz, and J. F. Bille, "Objective measurement of wave aberrations of the human eye with the use of a Hartmann–Shack wave-front sensor," J. Opt. Soc. Am. A **11**, 1949–1957 (1994).
5. W. T. Welford, *Aberrations of Optical Systems* (Hilger, Bristol, UK, 1986).
6. P. B. Kruger, S. Mathews, M. Katz, K. Aggarwala, and S. Nowbotsing, "Accommodation without feedback suggests directional signals specify ocular focus," Vision Res. **37**, 2511–2526 (1997).
7. A. Bradley, X. Zhang, and L. N. Thibos, "Achromatizing the human eye," Optom. Vision Sci. **68**, 608–616 (1991).
8. M. J. Collins, A. S. Goode, and D. A. Atchison, "Accommodation and spherical aberration," Invest. Ophthalmol. Visual Sci. Suppl. **38**, S1013 (1997).
9. D. L. Fridge, "Aberration synthesizer," J. Opt. Soc. Am. **50**, 87 (1960).
10. R. A. Buchroeder and R. B. Hooker, "Aberration generator," Appl. Opt. **14**, 2476–2479 (1975).
11. J. Liang, D. R. Williams, and D. T. Miller, "Supernormal vision and high-resolution retinal imaging through adaptive optics," J. Opt. Soc. Am. A **14**, 2884–2892 (1997).
12. F. Vargas-Martín, P. M. Prieto, and P. Artal, "Correction of the aberrations in the human eye with a liquid-crystal spatial light modulator: limits to performance," J. Opt. Soc. Am. A **15**, 2552–2562 (1998).
13. L. Alvarez, "Development of variable-focus lenses and a new refractor," J. Am. Optom. Assoc. **49**, 24–29 (1978).
14. R. Kingslake, "The interferometer patterns due to the primary aberrations," Trans. Ophthalmol. Soc. UK **27**, 94–99 (1925–1926).
15. D. Malacara, *Optical Shop Testing*, 2nd ed. (Wiley-Interscience, New York, 1991).
16. H. D. Crane and C. M. Steele, "Accurate three-dimensional eyetracker," Appl. Opt. **17**, 691–705 (1978).
17. B. Howland, "Use of crossed cylinder lens in photographic lens evaluation," Appl. Opt. **7**, 1587–1599 (1968).
18. B. Bourdoncle, J. P. Chauveau, and J. L. Mercier, "Traps in displaying optical performances of a progressive-addition lens," Appl. Opt. **31**, 3586–3593 (1992).
19. B. Howland and H. C. Howland, "Subjective measurement of high-order aberrations of the eye," Science **193**, 580–582 (1976).
20. G. Smith and D. A. Atchison, *The Eye and Visual Optical Instruments* (Cambridge U. Press, Cambridge, UK, 1997).